Two-photon autofluorescence microscopy of multicolor excitation

Dong Li, Wei Zheng, and Jianan Y. Qu*

Department of Electronic and Computer Engineering, Hong Kong University of Science and Technology,
Clear Water Bay, Kowloon, Hong Kong, China
*Corresponding author: eequ@ust.hk

We developed a two-photon autofluorescence lifetime imaging system with excitations selected from the supercontinuum generated from a photonic crystal fiber. The system excites multiple endogenous fluorophores, such as nicotinamide adenine dinucleotide (NADH) and tryptophan, simultaneously and produces coregistered two-photon autofluorescence images of a biological sample. The technology provides a unique approach to investigate the cellular metabolic activity and protein expression in cells that are potentially important for noninvasive precancer diagnostics. We demonstrated that by taking the tryptophan fluorescence as a reference the ratio of NADH to the tryptophan signal serves as a sensitive indicator of cellular metabolism. The ratio can also clearly differentiate normal cells from cancer cells. The tryptophan fluorescence lifetime images of cells shows that the lifetime of tryptophan fluorescence, varying over a wide range, may be highly dependent on the expression and structure of the protein that tryptophan is packed in. © 2009 Optical Society of America

OCIS codes: 180.4315, 320.6629, 300.6500, 300.6410, 170.3880.

Intrinsic fluorescence emission from the endogenous fluorophores provides the opportunity for noninvasive and label-free imaging of biological samples [1]. It is known that cellular nicotinamide adenine dinucleotide (NADH) fluorescence serves as an indicator of cellular aerobic and anaerobic metabolism, because it plays important roles in a variety of cellular metabolic pathways [2–4]. Tryptophan as well as tyrosine and phenylalanine are amino acids acting as building blocks in protein. Their fluorescence intensity and lifetime convey the information on protein content, protein structure, and changes in the cellular microenvironment [5,6]. It has been reported that NADH and tryptophan fluorescence signals could be used as the optical biomarkers for precancer detection [4,7]. This is because in the development of cancer, cells undergo a variety of transformations giving rise to increased metabolic activity, loss of cellular maturation, increased variability in nuclear shape and size, etc. In this Letter, we developed a time-resolved and spectrally resolved two-photon excited fluorescence (TPEF) microscope system for imaging of biological samples *in vivo* based on the excitation of multiple endogenous fluorophores simultaneously.

To maximally obtain the information on biochemistry and morphology of a biological sample, a TPEF imaging system based on intrinsic fluorescence emission should make use of the signals from multiple endogenous fluorophores. However, the two-photon excitation spectra of the endogenous fluorophores are significantly different from each other. For instance, the optimal excitation wavelengths for NADH and tryptophan are about 700 and 560 nm, respectively [8,9]. It requires an expensive femtosecond Ti:sapphire laser and optical parametric oscillator (OPO) system to generate two widely separated excitations [10]. To overcome the technical obstacle, we build a TPEF imaging system using supercontinuum generation of a photonic crystal fiber (PCF) as the ex-

citation source, as reported in [11–13]. A PCF is chosen to efficiently convert the energy of a femtosecond Ti:sapphire laser to the supercontinuum of a relatively narrow band covering the two-photon excitation wavelengths of NADH and tryptophan. The system produces NADH and tryptophan fluorescence lifetime images simultaneously. We demonstrate that the technology provides coregistered information on NADH and tryptophan in cells that could be potentially used for precancer diagnostics.

The schematic of the two-photon microscopy developed in this study is shown in Fig. 1. Briefly, a femtosecond Ti:sapphire laser tuned at 800 nm was used
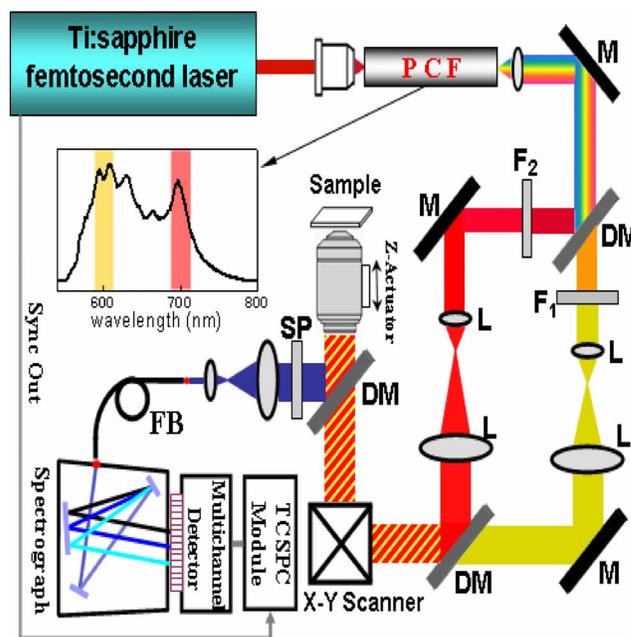

Fig. 1.   (Color online) Schematic of the TPEF imaging system of two-color excitation. PCF, photonic crystal fiber; M, mirror; DM, dichroic mirror; F1 and F2, bandpass filters; FB: fiber bundle; SP, shortpass filter; L, lens.

© 2009 Optical Society of America

to pump a 12-cm-long PCF (NL-1.4-775, Crystal Fiber). The inset in the figure shows the short wavelength band of the supercontinuum generated from the PCF. The fluctuation of the supercontinuum spectrum was found to be within 1.5% and negligible, as reported in [11]. A dichroic mirror of 650 nm was used to separate the supercontinuum into two-color beams. A 600 nm bandpass filter of 40 nm bandwidth was used to purify the excitation for tryptophan fluorescence and minimize the excitation of tyrosine and phenylalanine. A 700 nm bandpass filter of 40 nm bandwidth was used to select the excitation of NADH signal. The tryptophan and NADH excitation beams were combined together using another 650 nm dichroic mirror. A water-immersion 1.15 NA objective lens with high transmission in UV was used to focus the excitation beams into the examined sample and collect the backscattered fluorescence signals. A 60 $\times 60$ μm sampling area in sample was created by scanning a pair of galvo mirrors. The excitation powers at 600 and 700 nm bands on the sample were about 6 and 8 mW, respectively. This power ratio was maintained over the period of this study by controlling the pump power and coupling. The depth scanning was controlled by an actuator. A dichroic mirror of 510 nm was placed above the objective to reflect the TPEF signals to the detection channel. After passing through the short-pass filters of the cutoff wavelength at 532 nm, the TPEF signals were relayed by a telescope to a circle-to-line fiber bundle formed with 37 single fibers of 0.12 NA and 400 μm diameter. The fiber bundle conducted the TPEF signals to a spectrograph. A 16 photomultiplier tube array and a time-correlated single photon counting (TCSPC) module (PML-16 and SPC-150, Becker and Hickl GmbH) were used for the measurement of spectrally and time-resolved TPEF signals of the imaged sample. The TPEF were recorded in the wavelength range from 310 to 510 nm with about a 15 nm resolution. The samples used in this study were monolayer cultured SiHa and ECT1 cells; the cell lines were established from cancerous and normal cervical tissues, respectively. The acquisition time for a lifetime image of 128×128 pixels was 128 s, comparable to the measurement using femtosecond laser as excitation [14]. The systems produced lateral and axial resolutions of about 0.4 and 1.5 μm, respectively.

The TPEF spectra measured from a SiHa cell culture are presented in Figs. 2(a) and 2(b). For the comparison, the TPEF spectra measured from tryptophan and NADH solutions are also shown in the figures. The fluorescence of tyrosine and phenylalanine require the excitation of a wavelength shorter than tryptophan [5]. In this study, we did not observe the TPEF emission from tyrosine and phenylalanine solutions at 600 nm excitation. Therefore, the cellular fluorescence excited at 600 and 700 nm are dominated by tryptophan and NADH signals. As can be seen in the figure, both cellular TPEF spectra excited at 600 and 700 nm are slightly different from those measured from solutions. This may be because a large portion of the endogenous fluorophores are bound to proteins and enzymes in the cell [3]. The
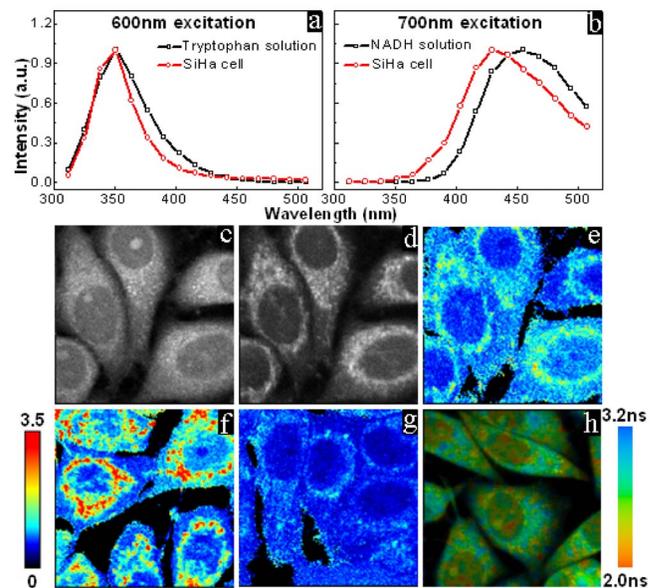

Fig. 2. (Color online) Representative TPEF spectra and images. a, Spectra of tryptophan solution and SiHa cells at 600 nm excitation; b, spectra of free NADH solution and SiHa cells at 700 nm excitation; c, tryptophan fluorescence image of SiHa cells; d, NADH fluorescence image of SiHa cells; e, ratio image of NADH to tryptophan fluorescence for control sample of SiHa cells; f, ratio image of SiHa cells treated with NaCN; g, ratio image of SiHa cells treated with CCCP; h, tryptophan fluorescence average lifetime image of SiHa cells.

cellular tryptophan and NADH fluorescence images acquired simultaneously from the SiHa cell sample are shown in Figs. 2(c) and 2(d). In Fig. 2(c), the protein-rich nucleolus exhibits strong tryptophan fluorescence. As expected, tryptophan signals in the cytoplasm are localized preferentially within protein-rich organelles, such as the endoplasmic reticulum [6]. The bright spots in the cytoplasm may be due to the protein aggregation that occurred in the endoplasmic reticulum. In Fig. 2(d) the bright spots and strips are the NADH fluorescence signals from mitochondria that are rich in NADH [4,14].

Though the change of NADH fluorescence is associated with cellular metabolism, it is challenging to use the NADH signal as a metabolic indicator directly, because the fluorescence intensity could be influenced by a variety of measurement conditions, such as the excitation power, optics alignment, etc. It is noted that the change of the cellular protein content is a slow process in the cell [15]. Therefore, the tryptophan fluorescence, an indicator of protein content, could be used as a reference to normalize out the variation in the excitation condition and quantify the change of NADH fluorescence when the cellular metabolism changes. In this study, the cellular metabolism of cell samples was manipulated by treating the cells with a mitochondrial inhibitor (NaCN) and uncoupler carbonyl cyanide 3-chlorophenylhydrazene (CCCP) as in a previous study [3,14]. Under the same excitation condition, we found that the tryptophan fluorescence of cells remained almost unchanged, while NADH signals changes significantly before and after the treatments. The ratio images of NADH over

tryptophan fluorescence before and after the treatment are shown in Figs. 2(e)–2(g). The color bar presents the ratio in the range from 0 to 3.5. Approximately a 46% increase of the ratio value in mitochondrial regions was observed from the cells treated with the mitochondrial inhibitor, while the ratio value decreased about 37% after treatment with the mitochondrial uncoupler. The results demonstrate that the ratio of NADH over tryptophan could be used as a sensitive indicator of metabolism in the imaging of live cells and tissue.

To understand the changes of NADH in a cell induced by the treatments, we extract the free NADH and protein-bound NADH signals from the time-resolved NADH fluorescence by using fitting analysis [3,14]. A dual-exponential function, $A_1 \exp(-t/\tau_1) + A_2 \exp(-t/\tau_2)$, was used to fit the time decay of NADH fluorescence. The short- and long-lifetime terms are dominated by free NADH and protein-bound NADH signals, respectively. The intensity ratio of NADH in free and bound forms to the tryptophan signal is listed in Table 1. The method to calculate the ratio values in mitochondrial, cytosolic, and nuclear compartments was described in a previous work [14]. As can be seen, the inhibitor and uncoupler mainly affect the concentration of the free NADH pool. A significant increase of the NADH signal after treatment with NaCN may be due to the accumulation of free NADH in mitochondria, while the treatment of CCCP causes a decrease of the NADH signal in three compartments because of the increased consumption of free NADH [14]. Finally, we found that the ratio of free NADH over the tryptophan signal in the ECT1 cell is significantly lower than the control SiHa cell, suggesting that the ratio could be used as a biomarker to differentiate a normal cell from a cancerous cell. This may be due to the loss of binding sites for NADH in malignant cells [16].

To study the temporal characteristics of tryptophan fluorescence, we fit the fluorescence lifetime signals using single and multiple exponential models. The lifetime of tryptophan in a solution calculated by using a single exponential function is about 2.4 ns, consistent with the previously reported results [17]. The tryptophan fluorescence lifetime image of the SiHa cell sample is shown in Fig. 2(h). The color bar presents the lifetime in the range from 2.0 to 3.2 ns. The fluorescence lifetime image was created based on pixel-by-pixel fitting analysis. A 3 × 3 pixel binning was used to achieve accurate fitting. Unlike the measurement in the tryptophan solution, the lifetime of cellular tryptophan fluorescence is distributed in a wide range. The lifetime varies significantly over the whole cellular region. This indicates that the lifetime of tryptophan fluorescence may be highly dependent on the expression, structure, and microenvironment of the protein that tryptophan is packed in.

Finally, it should be noted that with the appropriate optical filters and dichroic mirrors, the pump laser could be easily added as an additional excitation to generate a TPEF image of cellular flavin adenine dinucleotide emission and achieve a TPEF imaging of three-color excitation.

Table 1. Ratio of NADH to Tryptophan Fluorescence Signal[a–c]

		$I^{\text{free}}_{\text{NADH}}/I_{\text{tryptophan}}$			$I^{\text{bound}}_{\text{NADH}}/I_{\text{tryptophan}}$		
		M	C	N	M	C	N
SiHa	Control	0.82	0.53	0.50	1.64	0.99	0.99
	NaCN	1.55	0.56	0.54	2.28	1.01	0.92
	CCCP	0.48	0.43	0.36	1.28	0.97	0.97
ECT1	Control	0.56	0.34	0.27	1.65	0.95	0.88

[a]M, mitochondria; C, cytosol; N, nucleus.

[b]Ratios are calculated based on the short- and long-lifetime NADH fluorescence components in the 430–470 nm wavelength band to tryptophan fluorescence in the 340–360 nm wavelength band.

[c]The values of all parameters are based on the average over five measurements from at least three different samples. Maximal error is 10%.

References

1. G. A. Wagnieres, W. M. Star, and B. C. Wilson, Photochem. Photobiol. **68**, 603 (1998).
2. B. Chance, P. Cohen, F. Jobsis, and B. Schoener, Science **137**, 499 (1962).
3. Y. Wu, W. Zheng, and J. Y. Qu, Opt. Lett. **31**, 3122 (2006).
4. M. C. Skala, K. M. Riching, A. G. Fitzpatrick, J. Eickhoff, K. W. Eliceiri, J. G. White, and N. Ramanujam, Proc. Natl. Acad. Sci. USA **104**, 19494 (2007).
5. J. R. Lakowicz, *Principles of Fluorescence Spectroscopy*, 2nd ed. (Kluwer Academic/Plenum, 1999).
6. C. Mujat, C. Greiner, A. Baldwin, J. M. Levitt, F. Tian, L. A. Stucenski, M. Hunter, Y. L. Kim, V. Backman, M. Feld, K. Munger, and I. Georgakoudi, Int. J. Cancer **122**, 363 (2008).
7. P. Diagaradjane, M. A. Yaseen, J. Yu, M. S. Wong, and B. Anvari, Lasers Surg. Med. **37**, 382 (2005).
8. S. Huang, A. A. Heikal, and W. W. Webb, Biophys. J. **82**, 2811 (2002).
9. A. A. Rehms and P. R. Callis, Chem. Phys. Lett. **208**, 276 (1993).
10. F. J. Kao, Microsc. Res. Tech. **63**, 175 (2004).
11. K. M. Hilligsoe, T. V. Andersen, H. N. Paulsen, C. K. Nielsen, and K. Molmer, Opt. Express **12**, 1045 (2004).
12. K. Isobe, W. Watanabe, S. Matsunaga, T. Higashi, K. Fukui, and K. Itoh, Jpn. J. Appl. Phys. Part 2 **44**, L167 (2005).
13. J. A. Palero, V. O. Boer, J. C. Vijverberg, H. C. Gerritsen, and H. J. C. M. Sterenborg, Opt. Express **13**, 5363 (2005).
14. D. Li, W. Zheng, and J. Y. Qu, Opt. Lett. **33**, 2365 (2008).
15. B. Alberts, *Essential Cell Biology* (Garland Science, 2004).
16. A. C. Croce, A. Spano, D. Locatelli, S. Barni, L. Sciola, and G. Bottiroli, Photochem. Photobiol. **69**, 364 (1999).
17. S. Quentmeier, S. Denicke, J. E. Ehlers, R. A. Niesner, and K. H. Gericke, J. Phys. Chem. B **112**, 5768 (2008).